

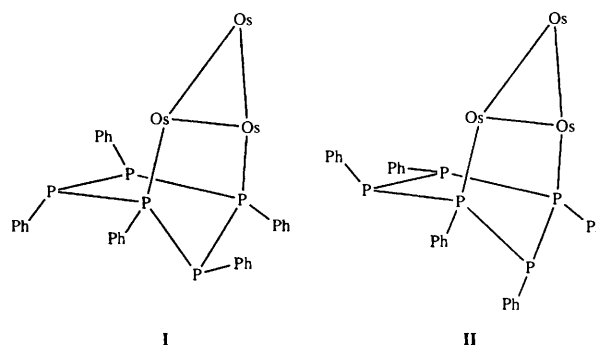
Structural and two-dimensional phosphorus-31 nuclear magnetic resonance studies of derivatives from (RP)₅ (R = Et or Ph) and activated triosmium clusters [Os₃(CO)₁₀X₂] (X = μ-H or NCMe)

How-Ghee Ang,* Siau-Gek Ang and Qi Zhang

Department of Chemistry, National University of Singapore, Lower Kent Ridge Road, Singapore 0511, Singapore

The reaction of the cyclophosphane (EtP)₅ with the activated triosmium cluster [Os₃(μ-H)₂(CO)₁₀] at 80 °C gave [Os₃(μ-H)(CO)₈(μ-η³-P₅Et₅H)] **1** and [Os₃(CO)₁₀{1,3-(PEt)₅}] **2**. The compound (PhP)₅ reacted with [Os₃(μ-H)₂(CO)₁₀] at room temperature to give [Os₃(μ-H)(CO)₈(μ-η³-P₅Ph₅H)] **3**. Treatment of (EtP)₅ with [Os₃(CO)₁₀(NCMe)₂] at room temperature afforded [Os₃(CO)₁₀{1,2-(PEt)₅}] **4**, while the reaction at 80 °C yielded only **2**. All the reaction products have been characterized by elemental analysis and IR, ¹H and ³¹P NMR spectroscopy. The solid-state structures of compounds **1**, **2** and **4** established by single-crystal X-ray diffraction showed that the phosphorus ring in **1** has undergone one P–P bond cleavage while those in **2** and **4** are intact. The solution structure of **3** has been fully characterized by two-dimensional ³¹P NMR spectroscopy.

Studies on the reactions of homocyclic phosphanes with a variety of metal carbonyls have shown that cyclophosphanes undergo ring-size change and form a variety of bridging groups at different ring positions.¹ Ang and co-workers^{2,3} found that the cyclopentaphosphanes (PhP)₅ and (MeP)₅ react with the hexacarbonyls of chromium, molybdenum and tungsten to yield compounds of the type [M(CO)_n{(PR)₅}] (n = 5–3) in which the (RP)₅ moiety is reported as a mono-, bi- and tridentate ligand, respectively. From the results of pyrolysis reactions of (RP)₅ (R = Ph, Et or Me), with [Fe(CO)₅] it appears that ring contraction always takes place to afford [Fe₂(CO)₃{(PR)₄}] in which (RP)₄ is a four-membered chain.^{3,4} However, few papers have concerned the coordination chemistry with transition-metal carbonyl clusters where cyclophosphanes ligate intact or phosphorus ring fission occurs to afford a phosphido group which stabilizes the clusters formed. Tetrameric (tBuP)₄ was recently reported to react with ruthenium carbonyl clusters under forcing conditions to give a number of phosphido- and phosphinidene-substituted ruthenium carbonyl clusters, indicating extensive disruption of the cyclic phosphorus ring.^{5,6} We found that the thermolyses of pentameric cyclophosphane, (PhP)₅, and tetrameric cyclophosphane, (F₃CP)₄, with ruthenium or osmium carbonyl clusters gave rise to not only phosphido groups, but also rare diphosphene fragments in several interesting cluster structures.^{7,8} On the other hand, we have also reported that the reactions of (PhP)₅ with activated triosmium or triruthenium carbonyl clusters afforded several cluster derivatives in which the ring remains intact.⁹ For instance, a pair of inversion isomers **I** and **II**, with formula [Os₃(CO)₁₀{1,3-(PPh)₅}] was obtained from the reaction of (PhP)₅ with the activated triosmium cluster [Os₃(CO)₁₀(NCMe)₂].⁹ The solution NMR data of these derivatives yielded a lot of useful information on the cyclophosphane structure. As an in-depth extension of this investigation, we report here the preparation and characterization of four new triosmium clusters **1–4** obtained from reactions of the cyclophosphanes (RP)₅ (R = Et or Ph), with the activated triosmium carbonyl clusters [Os₃(CO)₁₀X₂] (X = μ-H or NCMe). The phosphorus ring undergoes one P–P bond cleavage in **1** and **3**, but remains intact in **2** and **4**.



Results and Discussion

Preparation and characterization of compounds **1** and **2**

The reaction of (EtP)₅ with 1 mol equivalent of [Os₃(μ-H)₂(CO)₁₀] in CH₂Cl₂ at 80 °C overnight gave an orange mixture which afforded [Os₃(μ-H)(CO)₈(μ-η³-P₅Et₅H)] **1** (44%) and [Os₃(CO)₁₀{1,3-(PEt)₅}] **2** (30%) when subjected to thin-layer chromatography (TLC). Characterization data are given in Tables 1 and 2. The reaction at room temperature gave a brownish yellow solution which could not be resolved by TLC. The ¹H NMR spectrum of **1** shows multiplets at δ 6.05 and –17.85 due to a proton attached to P(1) and a bridging hydride bonded to Os atoms. The ³¹P-¹H NMR spectrum exhibits five multiplets at δ 21.6, –14.1, –49.5, –49.6 and –71.0. The proton-coupled ³¹P NMR spectrum shows that the phosphorus atom having the ³¹P NMR signal at δ –71.0 is linked to a proton with coupling constant 342 Hz. Through two-dimensional correlation (COSY-45) ³¹P-¹H NMR spectroscopy, the remaining signals at δ 21.6, –14.1, –49.5, –49.6 are assigned to P(2), P(5), P(4) and P(3) respectively.

The structure of compound **1** was determined by single-crystal X-ray diffraction (Fig. 1). Selected bond lengths and angles are listed in Table 3. The cleaved cyclophosphane ligand behaves as a tridentate donor co-ordinating to all three osmium atoms of the cluster. Atom P(5) bridges the edge Os(1)–Os(3) almost symmetrically; the Os(1)–P(5) distance [2.384(4) Å] is

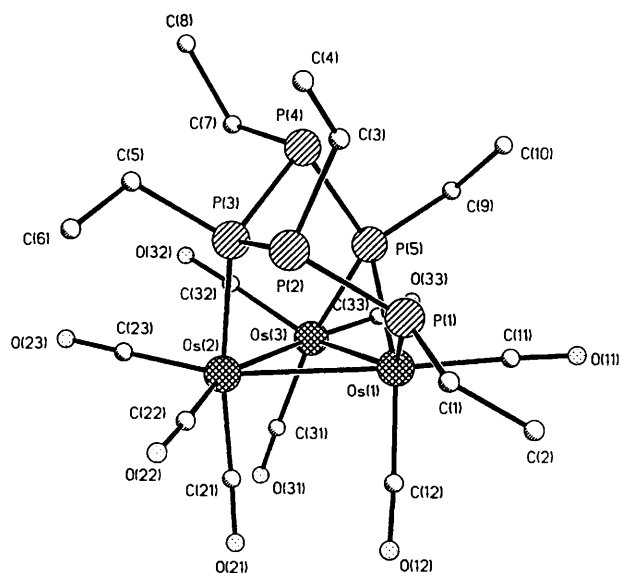
Table 1 Infrared data in the carbonyl region and elemental analysis data for compounds 1–4

Compound	$\nu(\text{CO})^a/\text{cm}^{-1}$	Analysis ^b (%)		
		C	H	P
1 $[\text{Os}_3(\mu\text{-H})(\text{CO})_8(\mu\text{-}\eta^3\text{-P}_3\text{Et}_3\text{H})]$	2066s, 2022s, 2014m, 2001m, 1995vs, 1969w, 1940w	19.90 (19.70)	2.20 (2.55)	12.50 (14.10)
2 $[\text{Os}_3(\text{CO})_{10}\{1,3\text{-}(\text{PEt})_5\}]$	2095s, 2059vw, 2027w, 2012s, 1980w, 1954w, 1949w	21.00 (20.85)	2.20 (2.15)	13.35 (13.45)
3 $[\text{Os}_3(\mu\text{-H})(\text{CO})_8(\mu\text{-}\eta^3\text{-P}_3\text{Ph}_5\text{H})]$	2069s, 2025s, 2001vs, 1980w, 1948m, 1937w	34.60 (34.10)	2.10 (2.00)	10.35 (11.60)
4 $[\text{Os}_3(\text{CO})_{10}\{1,2\text{-}(\text{PEt})_5\}]$	2096s, 2034m, 2018s, 2012vs, 1979m, 1962w, 1949m	20.90 (20.85)	2.00 (2.15)	13.30 (13.45)

^a Recorded in cyclohexane. ^b Calculated values given in parentheses.

Table 2 NMR data of compounds 1–4

Compound	³¹ P (δ , J/Hz)	¹ H (δ , J/Hz)
1	21.6 [m, P(2), $J(\text{P}^1\text{P}^2) = 198.1$, $J(\text{P}^2\text{P}^3) = 167.1$, $J(\text{P}^2\text{P}^4) = 39.5$] –14.1 [m, P(5), $J(\text{P}^4\text{P}^5) = 132.1$, $J(\text{P}^3\text{P}^5) = 28.4$] –49.5 [m, P(4), $J(\text{P}^3\text{P}^4) = 213.2$] –49.6 [m, P(3), $J(\text{P}^1\text{P}^3) = 16.1$] –71.0 [m, P(1)]	6.05 [m, 1 H, $J(\text{HP}) = 342.0$] 2.26 (m, CH ₂) 1.32 (m, CH ₃) –17.85 [m, 1 H, $J(\text{HP}) = 22.8$]
2	54.8 [m, P(1), $J(\text{P}^1\text{P}^2) = 256.4$, $J(\text{P}^1\text{P}^5) = 233.8$, $J(\text{P}^1\text{P}^3) = 20.1$, $J(\text{P}^1\text{P}^4) = 15.4$] 34.8 [m, P(4), $J(\text{P}^4\text{P}^5) = 248.0$, $J(\text{P}^3\text{P}^4) = 240.9$, $J(\text{P}^2\text{P}^4) = 12.6$] 2.5 [m, P(3), $J(\text{P}^2\text{P}^3) = 312.5$, $J(\text{P}^3\text{P}^5) = 7.0$] –15.3 [m, P(2), $J(\text{P}^2\text{P}^5) = 53.3$] –24.9 [m, P(5)]	2.29 (m, CH ₂) 1.31 (m, CH ₃)
3	56.1 [m, P(2), $J(\text{P}^1\text{P}^2) = 241.4$, $J(\text{P}^2\text{P}^3) = 230.1$, $J(\text{P}^2\text{P}^4) = 6.3$] –15.8 [m, P(5), $J(\text{P}^4\text{P}^5) = 251.0$, $J(\text{P}^3\text{P}^5) = 127.4$, $J(\text{P}^1\text{P}^5) = 26.9$] –19.6 [m, P(4), $J(\text{P}^3\text{P}^4) = 229.9$, $J(\text{P}^1\text{P}^4) = 33.0$] –49.2 [m, P(3), $J(\text{P}^1\text{P}^3) = 42.5$] –76.6 [m, P(1), $J(\text{P}^1\text{H}) = 366.1$]	8.43 [d, 1 H, $J(\text{HP}) = 366.1$] –17.48 [m, 1 H, $J(\text{HP}) = 23.1$]
4	8.3 [m, P(3), P(4), P(5)] –71.64 [m, P(1), P(2)]	2.25 (m, CH ₂) 1.30 (m, CH ₃)

**Fig. 1** Molecular structure of $[\text{Os}_3(\mu\text{-H})(\text{CO})_8(\mu\text{-}\eta^3\text{-P}_3\text{Et}_3\text{H})]$ 1

similar to that [2.373(4) Å] of Os(3)–P(5). Atoms P(1) and P(3) bond *via* axial sites to Os(1) and Os(2) respectively. The Os(1)–P(1) distance [2.304(6) Å] is much shorter than that [2.400(4) Å] of Os(2)–P(3). The P–P distances (2.179–2.190 Å) are shorter than the average (2.22 Å) found in $(\text{PhP})_5$,¹⁰ $(\text{F}_3\text{CP})_5$ ¹¹ and $(\text{F}_3\text{CP})_4$,¹² with the exception of P(2)–P(3) [2.220(7) Å]. The three osmiums form an approximately isosceles triangle in which the side-edge is 2.916(2) Å and the bottom-edge 2.861 Å. The proton bound to P(1) was located by proton-coupled ³¹P NMR spectroscopy. The bridging hydrogen was found by two-dimensional ¹H–³¹P NMR correlation

Table 3 Selected bond lengths (Å) and angles (°) of compound 1

Os(1)–Os(2)	2.861(2)	P(4)–P(5)	2.180(5)
Os(2)–Os(3)	2.912(2)	Os(1)–P(1)	2.304(6)
Os(1)–O(3)	2.919(2)	Os(1)–P(5)	2.384(4)
P(1)–P(2)	2.179(7)	Os(2)–P(3)	2.400(4)
P(2)–P(3)	2.220(7)	Os(3)–P(5)	2.374(4)
P(3)–P(4)	2.190(6)		
Os–C (mean)	1.917	C–O (mean)	1.135
P–P (mean)	2.192	P–C (mean)	1.826
Os(2)–Os(1)–Os(3)	59.9(1)	Os(1)–Os(2)–Os(3)	60.4(1)
Os(1)–Os(3)–Os(2)	59.7(1)	P(1)–P(2)–P(3)	94.5(3)
P(2)–P(3)–P(4)	105.7(2)	P(3)–P(4)–P(5)	88.6(2)
P–P–P (mean)	92.3		
Os(1)–P(1)–P(2)	119.1(3)	P(1)–Os(1)–P(5)	96.7(7)
Os(1)–P(5)–P(4)	120.1(2)	Os(3)–P(5)–P(4)	123.2(2)
Os(1)–P(5)–Os(3)	75.7(1)	P(5)–Os(1)–Os(3)	52.0(1)
P(5)–Os(1)–Os(3)	52.3(1)	Os(1)–Os(2)–P(3)	83.5(1)
Os(3)–Os(2)–P(5)	98.2(1)	P(2)–P(3)–Os(2)	108.2(2)
P(4)–P(3)–Os(2)	119.2(2)		

spectroscopy to lie across the Os(1)–Os(3) edge, opposite the bridging atom P(5). The trisodium system contains 54 electrons.

The carbonyl region of the IR spectrum for compound 2 is quite similar to that of $[\text{Os}_3(\text{CO})_{10}\{1,3\text{-}(\text{PPh})_5\}]$ II. The ¹H NMR spectrum shows multiplets at δ 2.29 and 1.31 due to the CH₂ and CH₃ of ethyl groups. The ³¹P NMR spectrum exhibits a perfect first-order spin pattern with relative intensities of 1:1:1:1:1 (Fig. 2). In the COSY-45 ³¹P NMR spectrum each resonance shows two ¹J cross-peaks due to strong coupling between bound phosphorus neighbours, while the remaining positively tilted cross-peaks are attributed to the two-bond

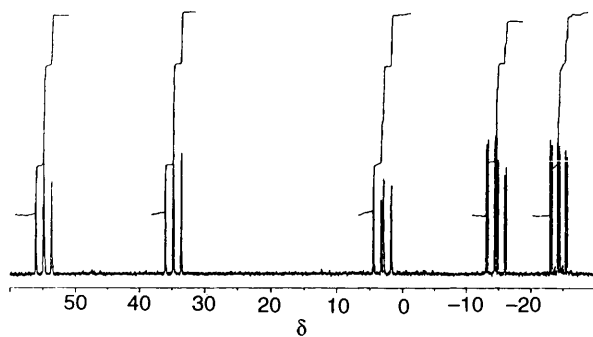


Fig. 2 The $^{31}\text{P}\{-^1\text{H}\}$ NMR spectrum of compound **2**

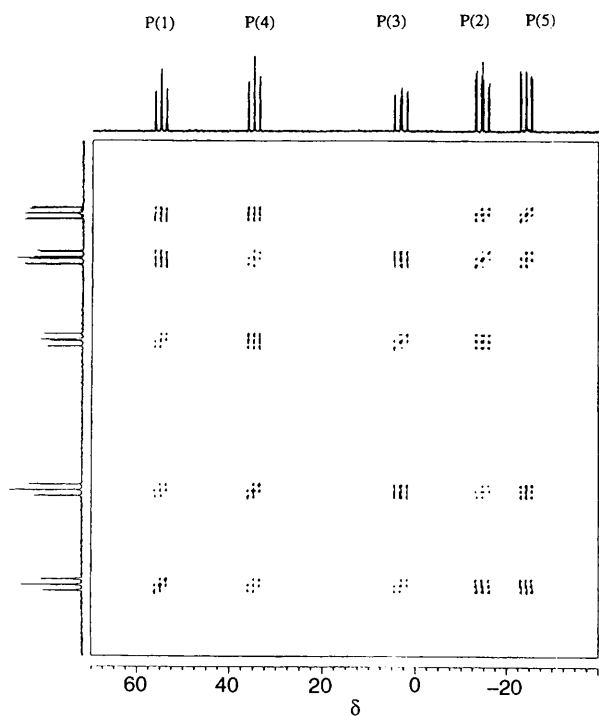


Fig. 3 Two-dimensional (COSY-45) $^{31}\text{P}\{-^1\text{H}\}$ NMR spectrum of compound **2**

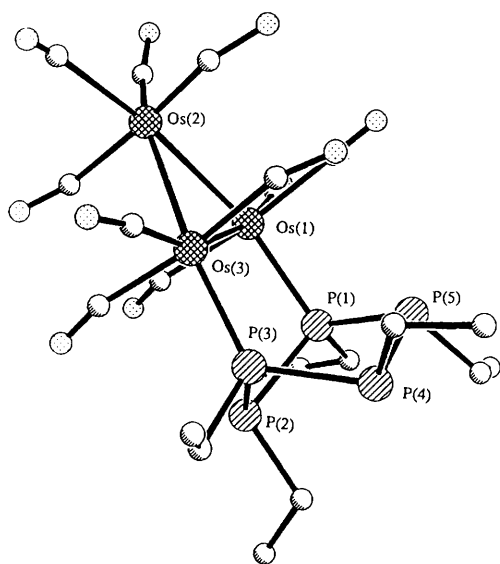


Fig. 4 Molecular structure of $[\text{Os}_3(\text{CO})_{10}\{1,3\text{-(PEt)}_5\}_2]$ **2**

phosphorus interactions.¹³ This, together with the magnitudes of the coupling constants, allows the assignment of the ^{31}P signals as shown in Fig. 3.

Table 4 Selected bond lengths (Å) and angles (°) of compound **2**

Os(1)–Os(2)	2.887(8)	P(1)–P(5)	2.25(2)
Os(2)–Os(3)	2.899(8)	Os(1)–P(1)	2.33(1)
Os(1)–O(3)	2.893(8)	Os(3)–P(3)	2.33(1)
P(1)–P(2)	2.23(2)	Os–C (mean)	1.907
P(2)–P(3)	2.23(2)	P–C (mean)	1.913
P(3)–P(4)	2.24(2)	C–O (mean)	1.238
P(4)–P(5)	2.23(2)		
Os(2)–Os(1)–Os(3)	58.8(2)	Os(1)–Os(2)–Os(3)	60.0(2)
Os(1)–Os(3)–Os(2)	60.2(2)	P(2)–P(1)–P(5)	108.1(4)
P(1)–P(2)–P(3)	87.8(4)	P(2)–P(3)–P(4)	98.1(4)
P(3)–P(4)–P(5)	96.6(5)	P(1)–P(5)–P(4)	100.6(4)

The molecular structure of compound **2** was determined by single-crystal X-ray diffraction (Fig. 4). Selected bond lengths and angles are given in Table 4. The structure is similar to that of $[\text{Os}_3(\text{CO})_{10}\{1,3\text{-(PPh)}_5\}_2]$ **II** where the intact $(\text{EtP})_5$ acts as a bidentate ligand, taking up two equatorial sites of the osmium triangular plane through two P atoms in the 1,3 positions of the phosphorus ring. The smallest angle, P(1)–P(2)–P(3) 87.4°, is much smaller than the other P–P–P angles because the two phosphorus atoms at positions 1 and 3 must move closer to fit the short Os–Os bond in the triosmium cluster.

Preparation and characterization of compound **3**

The compound $(\text{PhP})_5$ reacted with $[\text{Os}_3(\mu\text{-H})_2(\text{CO})_{10}]$ in CH_2Cl_2 at room temperature overnight to afford an orange solution which gave cluster $[\text{Os}_3(\text{CO})_{10}\{1,3\text{-(PPh)}_5\}_2]$ **I** (12%) and a new cluster $[\text{Os}_3(\mu\text{-H})(\text{CO})_8(\mu\text{-}\eta^3\text{-P}_5\text{Ph}_5\text{H})]$ **3** (13%) when subjected to thin-layer chromatography (TLC). The reaction at 80 °C gave $[\text{Os}_3(\text{CO})_{10}\{1,3\text{-(PPh)}_5\}_2]$ **I** (9%) and a mixture (ca. 66%) of **3** and $[\text{Os}_3(\text{CO})_{10}\{1,3\text{-(PPh)}_5\}_2]$ **II** which was formed from its inversion isomer **I**. The compounds **3** and **II** are difficult to separate using TLC, having similar R_f values. Clusters **I** and **II** were shown spectroscopically to be the same as the compounds formed previously by the reaction of $(\text{PhP})_5$ with $[\text{Os}_3(\text{CO})_{10}(\text{NCMe})_2]$ at 80 °C. Elemental analysis and IR spectral studies indicate that **3** has a structure similar to that of **1**, as shown in Fig. 5. It was characterized by ^1H , one-dimensional ^{31}P and two-dimensional $^{31}\text{P}\text{-}^{31}\text{P}$ (COSY-45) and $^1\text{H}\text{-}^{31}\text{P}$ heteronuclear shift correlation NMR spectroscopy. The ^1H NMR spectrum shows resonances at δ 8.43 (d), 7.53 (m) and -17.48 (m) due to a proton directly attached to a phosphorus atom, phenyl protons and a bridging hydride, respectively. The $^{31}\text{P}\{-^1\text{H}\}$ NMR spectrum shows five signals with relative intensities of 1:1:1:1:2. The relative intensity of the phosphorus signal at δ -76.6 can be attributed to the nuclear Overhauser effect. The proton-coupled ^{31}P NMR spectrum exhibits five signals with relative intensities of 1:1:1:1:1 and $J(\text{PH})$ of 366.1 Hz. It also confirmed that the phosphorus atom with signal at δ -76.6 was attached to a proton. The COSY-45 ^{31}P NMR spectrum then allows the assignments of the other resonances (Fig. 6). Cross-peaks for neighbouring phosphorus atoms are observed for P(1)–P(2), P(2)–P(3), P(3)–P(4) and P(4)–P(5). Long-range cross-peaks are found for P(1)–P(3) and P(3)–P(5), and even longer-range interactions between P(1)–P(4) and P(1)–P(5). The $^1\text{H}\text{-}^{31}\text{P}$ correlation NMR spectrum (Fig. 7) shows three significant cross-peaks between the bridging hydride and P(1), the bridging hydride and P(5), as well as the terminal proton and P(1).

Preparation and characterization of compound **4**

Treatment of $(\text{EtP})_5$ with the activated triosmium cluster $[\text{Os}_3(\text{CO})_{10}(\text{NCMe})_2]$ at room temperature overnight afforded a 1,2-substituted product **4** (17%) while reaction at 80 °C gave only the 1,3-substituted product **2** (7%). The yields of the

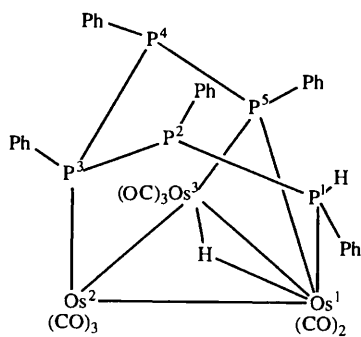


Fig. 5 Proposed structure of compound 3

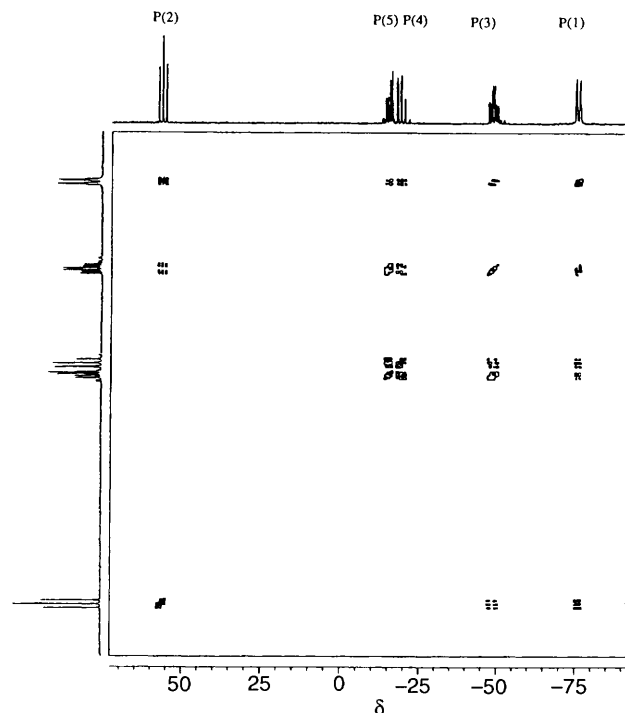


Fig. 6 Two-dimensional (COSY-45) $^{31}\text{P}\{-^1\text{H}\}$ NMR spectrum of compound 3

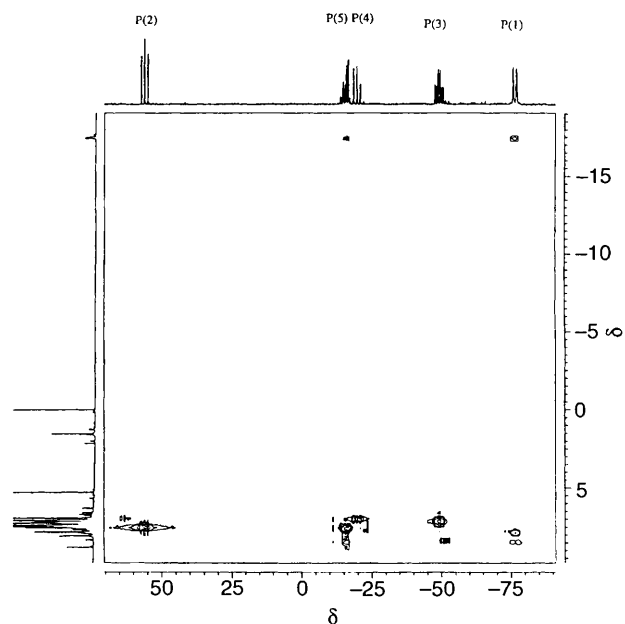


Fig. 7 Two-dimensional heteronuclear shift correlation $^{31}\text{P}\{-^1\text{H}\}$ NMR spectrum of compound 3

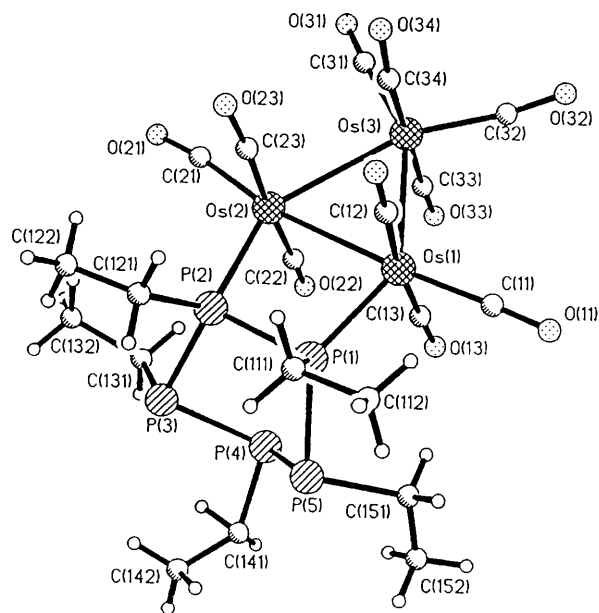


Fig. 8 Molecular structure of $[\text{Os}_3(\text{CO})_{10}\{1,2\text{-(PEt)}_5\}] \mathbf{4}$

reactions under different conditions are listed in Table 5. Compound **4**, which was formed at room temperature, was not stable and slowly decomposed at higher temperatures. As shown in Table 5, the yield of **4** at 50 °C is half that at room temperature. The compound was not obtained when the reaction was carried out at 80 °C overnight. The lower thermal stability of **4** was also observed through NMR spectroscopy where a pure sample was completely decomposed when heated at 80 °C overnight in an NMR tube. In contrast, higher temperature favours the formation of the 1,3-substituted product **2**. The latter was also obtained in almost 100% yield from the thermal transformation of $[\text{Os}_3(\text{CO})_{11}\{(\text{PEt})_5\}]^{14}$ in dichloromethane at 80 °C for 17 h. The ^{31}P NMR spectrum of **4** shows an AA'BXX' spin pattern with two multiplets at δ 8.33 and -71.64 in the ratio of 3:2, respectively.

The molecular structure of compound **4** was determined by single-crystal X-ray diffraction and is shown together with the atomic labelling scheme in Fig. 8. Selected bond lengths and angles are given in Table 6. The cyclophosphane (EtP)₅ acts as a bidentate ligand, taking up equatorial sites of the osmium triangular plane and chelating across an Os–Os edge, through two P atoms in the 1,2 positions of the phosphorus ring. This is the first example in cyclophosphane chemistry where chelation occurs *via* such positions. The small torsion angle (0.1°) of P(5)–P(1)–P(2)–P(3) indicates that the four atoms are in a plane. The four atoms Os(1), Os(2), P(2) and P(1) are also in a plane because the torsion angle (0.3°) of Os(1)–P(1)–P(2)–Os(2) is almost zero. The torsion angle (average 5.4°) of Os(3)–Os(2)–Os(1)–P(1) indicates that atom Os(3) is positioned slightly below the common plane of Os(1), Os(2), P(2) and P(1). Compound **4** possesses approximate *m* symmetry with the symmetry plane passing through Os(3), the midpoints of the Os(1)–Os(2) and P(1)–P(2) bonds, and P(4) (Fig. 9). It is also noteworthy that atoms P(1) and P(2) bonded to Os atoms are in an almost fully eclipsed conformation since the torsion angles are 0.3, -0.1 and -1.5° for Os(1)–P(1)–P(2)–Os(2), P(5)–P(1)–P(2)–P(3) and C(111)–P(1)–P(2)–C(121) respectively as seen in Fig. 10.

Experimental

The reactions described above were carried out under nitrogen in evacuated reaction tubes using vacuum-line techniques. All solvents were dried over appropriate drying agents¹⁵ and distilled prior to use. The compounds (PhP)₅, (EtP)₅, $[\text{Os}_3\text{-}$

$(\mu\text{-H})_2(\text{CO})_{10}]$ and $[\text{Os}_3(\text{CO})_{10}(\text{NCMe})_2]$ were prepared by literature methods.^{16–18} The products of the reactions were separated by thin-layer chromatography on 20×20 cm glass plates coated with 0.3 mm of Merck Kieselgel 60GF₂₅₄, using mixtures of dichloromethane and hexane in various proportions as eluents. Infrared spectra were recorded as solutions in 0.5 mm KBr cell on a Perkin-Elmer model 983G spectrophotometer. ¹H and ³¹P NMR spectra on Bruker 300 and 500 MHz

Fourier-transform spectrometers using SiMe₄ (¹H) and H₃PO₄ (³¹P) as references.

Synthesis

$[\text{Os}_3(\mu\text{-H})(\text{CO})_8(\mu\text{-}\eta^3\text{-P}_5\text{Et}_5\text{H})]$ **1** and $[\text{Os}_3(\text{CO})_{10}\{\text{1,3-(PEt)}_2\}]$ **2**. The compounds (EtP)₅ (0.058 g, 0.193 mmol), $[\text{Os}_3(\mu\text{-H})_2(\text{CO})_{10}]$ (0.165 g, 0.193 mmol) and dichloromethane (10 cm³) were mixed in a Carius tube and degassed *in vacuo*. The

Table 5 Yields (%) of compounds **2** and **4** under different reaction conditions

Condition	2	4
Room temperature, 17 h	0	17
80 °C, 17 h	7	0
80 °C, 2 h	7	10
50 °C, 10 h	11	9

Table 6 Selected bond lengths (Å) and angles (°) of compound **4**

Os(1)–Os(2)	2.881(8)	P(3)–P(4)	2.217(13)
Os(2)–Os(3)	2.890(8)	P(4)–P(5)	2.237(17)
Os(1)–Os(3)	2.899(8)	P(1)–P(5)	2.198(10)
P(1)–P(2)	2.204(12)	Os(1)–P(1)	2.334(8)
P(2)–P(3)	2.208(11)	Os(2)–P(2)	2.347(9)
Os–C (mean)	1.895	P–C (mean)	1.847
C–O (mean)	1.172		
Os(2)–Os(1)–Os(3)	60.0(2)	Os(1)–Os(2)–Os(3)	60.3(2)
Os(1)–Os(3)–Os(2)	59.7(2)	P(2)–P(1)–P(5)	104.7(4)
P(1)–P(2)–P(3)	103.8(4)	P(2)–P(3)–P(4)	95.2(4)
P(3)–P(4)–P(5)	95.2(5)	P(1)–P(5)–P(4)	94.7(4)
P(1)–Os(1)–C(12)	89.5(7)	P(1)–Os(1)–C(13)	97.0(7)
P(1)–Os(1)–Os(2)	81.9(2)	P(2)–Os(2)–C(23)	88.4(7)
P(2)–Os(2)–C(22)	95.2(6)	P(2)–Os(2)–Os(1)	81.4(2)
Os(1)–P(1)–P(2)	98.4(3)	Os(1)–P(1)–C(111)	116.9(3)
P(5)–P(1)–C(111)	101.0(3)	Os(2)–P(2)–P(1)	98.3(3)
Os(2)–P(3)–C(121)	119.5(3)	P(3)–P(2)–C(121)	100.9(3)
P(2)–P(3)–C(131)	102.8(4)	P(4)–P(3)–C(131)	97.5(5)
P(5)–P(4)–C(141)	96.6(5)	P(3)–P(4)–C(141)	100.9(4)
P(1)–P(5)–C(151)	102.6(4)	P(4)–P(5)–C(151)	100.1(4)

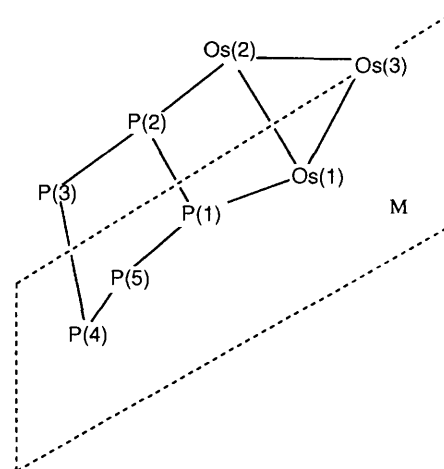


Fig. 9 Skeleton of compound **4**

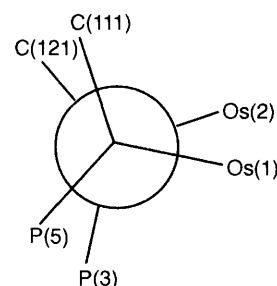


Fig. 10 Newman projection from P(1) to P(2) for compound **4**

Table 7 Crystal data and data collection parameters for compounds **1**, **2** and **4**

	1	2	4
Formula	C ₁₈ H ₂₅ O ₈ Os ₃ P ₅	C ₂₀ H ₂₅ O ₁₀ Os ₃ P ₅	C ₂₀ H ₂₅ O ₁₀ Os ₃ P ₅
<i>M</i>	1094.9	1150.8	1150.8
Colour, habit	Orange block	Yellow plate	Orange prism
Crystal size/mm	0.28 × 0.22 × 0.17	0.30 × 0.30 × 0.25	0.40 × 0.32 × 0.12
Crystal system	Monoclinic	Monoclinic	Triclinic
Space group	<i>C</i> 2/ <i>c</i>	<i>P</i> 2 ₁ / <i>c</i>	<i>P</i> $\bar{1}$
<i>a</i> Å	19.992(2)	10.62(3)	10.37(2)
<i>b</i> Å	10.204(4)	18.37(3)	11.20(3)
<i>c</i> Å	28.784(9)	17.39(4)	16.36(5)
α °			98.30(3)
β °	96.53(3)	106.420(0)	97.14(2)
γ °			117.55(5)
<i>V</i> Å ³	5834(2)	3254(11)	1628(8)
<i>Z</i>	8	4	2
<i>F</i> (000)	4000	2112	1056
<i>D</i> _c g cm ⁻³	2.493	2.349	2.348
μ (Mo-K α)/cm ⁻¹	133.47	119.75	119.71
2 θ Range/°	3.0–50.0	4.0–48.0	4.0–48.0
Scan speed/° min ⁻¹	3.00–16.74	3.08–29.30	6.00–20.00
Scan range/°	1.20	1.00 + K α separation	1.00
Total reflections	5166	5082	5266
Unique reflections	5014	5082	5065
Observed reflections [<i>F</i> > 4.0 σ (<i>F</i>)]	3426	2773	3272
No. refined parameters	308	193	315
<i>k</i> in $\omega^{-1} = \sigma^2(F) + kF^2$	0.0006	0.0010	0.0010
<i>R</i> (observed data)	0.0465	0.1028	0.0560
<i>R</i> ' (observed data)	0.0497	0.1615	0.0656
Goodness of fit	1.21	1.91	1.32

mixture was heated in an oven at 80 °C overnight. Excess of solvent was removed under vacuum. The residue was dissolved in dichloromethane (2 cm³) and subjected to TLC on silica using dichloromethane–hexane (3:7) as eluent. Orange crystalline compound **1** was extracted from band 1 and recrystallized from hexane at low temperature. Yield: 92 mg (44%). Yellow crystals of **2** extracted from band 2 were obtained from a mixture of dichloromethane and hexane at 0 °C. Yield: 66 mg (30%).

[Os₃(μ-H)(CO)₈(μ-η³-P₅Ph₅H)] **3**. The compound (PhP)₅ (0.127 g, 0.235 mmol) was added to a solution of [Os₃(μ-H)₂(CO)₁₀] (0.200 g, 0.235 mmol) in dichloromethane (10 cm³). The mixture was stirred at room temperature overnight, during which time it changed from dark purple to orange. The solvent was removed under vacuum and TLC of the residue using dichloromethane–hexane (3:7) as eluent afforded compound **3**. Yield: 43 mg (13%).

[Os₃(CO)₁₀{1,2-(PEt)₅}] **4**. The compound (EtP)₅ (0.67 g, 0.224 mmol) was added to a solution of [Os₃(CO)₁₀(NCMe)₂] (0.209 g, 0.224 mmol) in dichloromethane (10 cm³). The mixture was allowed to stir at room temperature overnight, during which time it changed from brown to orange. The solvent was removed under vacuum and TLC of the residue using dichloromethane–hexane (1:4) as eluent afforded compound **4**. Yield: 42 mg (17%).

Crystallography

Crystal data and details of measurements for clusters **1**, **2** and **4** are reported in Table 7. Diffraction intensities were collected at 298 K on a Siemens R3m/V diffractometer, using the ω-scan (for **1** and **4**) and 2θ–θ scan modes (for **2**) with graphite-monochromatized Mo-K_α radiation (λ = 0.71069 Å). All computations were carried out on a Micro VAX 2000 computer using the SHELXTL PLUS program package.¹⁹ The structures were solved by direct methods for the osmium atoms and Fourier-difference techniques for the remaining non-hydrogen atoms. Full-matrix least-squares refinement (on *F*) was performed with all non-hydrogen atoms anisotropic. An empirical (ψ-scan) correction was applied in each case.

Atomic coordinates, thermal parameters and bond lengths

and angles have been deposited at the Cambridge Crystallographic Data Centre (CCDC). See Instructions for Authors, *J. Chem. Soc., Dalton Trans.*, 1996, Issue 1. Any request to the CCDC for this material should quote the full literature citation and the reference number 186/85.

Acknowledgements

We thank the National University of Singapore for financial support and for a Research Scholarship (to Q. Z.).

References

- 1 B. O. West, in *Homoatomic Rings, Chains and Macromolecules of the Main Group Elements*, ed. A. L. Rheingold, Elsevier, Amsterdam, 1977, p. 409.
- 2 H. G. Ang, J. S. Shannon and B. O. West, *Chem. Commun.*, 1965, 10.
- 3 H. G. Ang and B. O. West, *Aust. J. Chem.*, 1967, **20**, 1133.
- 4 A. L. Rheingold and M. E. Foutain, *Organometallics*, 1984, **3**, 1417.
- 5 B. F. G. Johnson, T. M. Lauer, J. Lewis, P. R. Raithby and W. T. Wong, *J. Chem. Soc., Dalton Trans.*, 1993, 973.
- 6 E. Charalambous, L. Heuer, B. F. G. Johnson, J. Lewis, W. S. Li, M. McPartlin and A. D. Massey, *J. Organomet. Chem.*, 1994, **468**, C9.
- 7 H. G. Ang, K. W. Ang, S. G. Ang and W. L. Kwik, *14th International Symposium on Fluorine Chemistry*, Yokohama, 1994.
- 8 H. G. Ang, L. L. Koh and Q. Zhang, *J. Chem. Soc., Dalton Trans.*, 1995, 2757.
- 9 H. G. Ang, S. G. Ang, W. L. Kwik and Q. Zhang, *J. Organomet. Chem.*, 1994, **485**, C6.
- 10 J. J. Daly, *J. Chem. Soc.*, 1964, 6147.
- 11 C. J. Spencer and W. N. Lipscomb, *Acta Crystallogr.*, 1961, **14**, 250.
- 12 G. J. Palenik and J. Donohue, *Acta Crystallogr.*, 1962, **15**, 564.
- 13 J. Hahn, in *Phosphorus-31 NMR Spectroscopy in Stereochemical Analysis*, eds. J. G. Verkade and L. D. Quin, VCH, Deerfield Beach, Florida, 1987, ch. 10, p. 331.
- 14 H. G. Ang, S. G. Ang, W. L. Kwik and Q. Zhang, unpublished work.
- 15 D. F. Shriver and M. A. Dredzon, *The Manipulation of Air-sensitive Compounds*, 2nd edn., Wiley, New York, 1986.
- 16 H. G. Ang, Ph.D. Dissertation, Monash University, 1965.
- 17 H. D. Kaesz, *Inorg. Synth.*, 1989, **28**, 238.
- 18 S. R. Drake and R. Khattar, *Org. Synth.*, 1988, **14**, 24.
- 19 G. M. Sheldrick, Siemens, Madison, WI, 1986.

Received 17th January 1996; Paper 6/00374E